ACS Catalysis

Letter

pubs.acs.org/acscatalysis

Manganese-Modified Fe_3O_4 Microsphere Catalyst with Effective Active Phase of Forming Light Olefins from Syngas

Yi Liu,[†] Jian-Feng Chen,[†] Jun Bao,[‡] and Yi Zhang*[,†]

[†]State Key Laboratory of Organic−Inorganic Composites, Beijing University of Chemical Technology, Beijing 100029, China

[‡]National Synchrotron Radiation Laboratory & School of Nuclear Science and Technology, University of Science and Technology of China, Hefei, Anhui 230029, China

Supporting Information

ABSTRACT: A manganese-modified Fe_3O_4 microsphere catalyst was developed, which effectively converts the syngas to light olefins (C_2−C_4) with selectivity up to 60.1% in all hydrocarbon products. This nonporous catalytic material with fine dispersed manganese contributes to clarifying the different role of iron carbides by solely modifying the carburization of the catalysts and reducing the diffusion resistance of products. Combining various characterization results, including XAFS and Mössbauer spectroscopy, it is found that the electronic state of surface carbonaceous species was affected by the Mn promoter, leading to the formation of special iron carbide (θ-Fe_3C), and the reactivity for light olefins formation was highly dependent on the content of θ-Fe_3C.

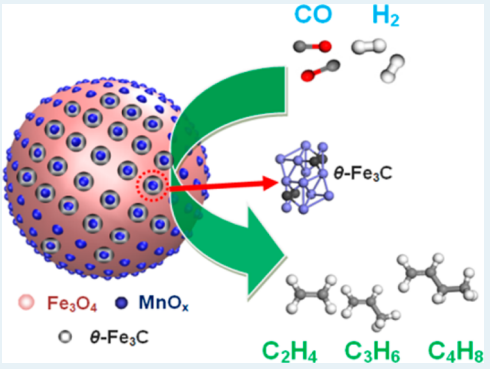

KEYWORDS: *iron microsphere, iron carbide, manganese, Fischer−Tropsch synthesis, light olefins*

Light olefins (C_2−C_4) are key building blocks of the chemical industry, and they are typically produced by steam cracking naphtha.[1] The direct conversion of syngas into light olefins via the Fischer−Tropsch synthesis (FTS) process is a promising route to meet the increasing demand for chemical feed-stocks.[2,3] In general, FTS products are almost normal aliphatic hydrocarbons, following the Anderson−Schultz−Flory (ASF) distribution, which is wide and unselective.[4] Therefore, the development of selective catalysts has attracted much attention.[5−10] Compared with other FTS catalysts, iron-based catalysts have great potential for selective formation of light olefins from FTS. It is well known that iron carbide is recognized as the active phase for the FTS reaction.[11] However, the activity and selectivity of different iron carbides is still unclear.

Many studies suggest that the reactivity of the iron-based FTS catalyst is correlated with the properties of iron carbides.[12−15] Therefore, maintaining a carburized surface and suitable carbides particle size are the main issues for designing effective iron-based FTS catalysts.[16] However, the iron carbides that would be formed during reduction and FTS reaction are more than one phase, such as the reported χ-Fe_5C_2 (Hägg carbide) and θ-Fe_3C (cementite) forms, as well as ε-$Fe_{2.2}C$, which was formed under special conditions.[16,17] Furthermore, the exact role of each iron carbide phase in the formation of light olefins remains unclear.

To date, manganese has been widely used as an efficient promoter for the FTS catalysts.[1,2,18−21] It was reported that the presence of Mn enhanced the selectivity of olefins and suppressed the formation of methane.[18,19] Manganese was also found to promote the dispersion of iron and make the catalysts less prone to deactivation.[20a] Sometimes an increase in intrinsic activity for the Mn-promoted Fe catalysts will be observed.[19c] In addition, many studies[18a,20a] found that a solid-solution compound has formed when Mn was added to the iron-based catalysts, resulting in the Mn-induced textural structure variation of the iron catalyst, which would change the particle size and reducibility of iron[20a] and the diffusion rate.[2,21] Meanwhile, the electronic state of the active phase would be influenced via the electronic transfer between iron and support.[22,23] Generally, these factors always interact with each other to influence the activity and selectivity of obtained catalysts in the FTS reaction. On the other hand, it is reported that primary α-olefins can be readsorbed to promote the secondary reactions.[24,25] Therefore, the diffusion rate would influence the selectivity of products and confuse the effects of promoter.

Herein, a manganese-modified Fe_3O_4 microsphere catalyst was developed, as illustrated in Figure 1a, where the MnO_x was dispersed on the surface of Fe_3O_4 microsphere to avoid the porous structure and solely modify the carburization of the catalysts. It was estimated that this newly designed catalyst would improve the selectivity of light olefins by alleviating secondary reactions and tuning the properties of surface

Received: March 8, 2015
Revised: April 19, 2015
Published: May 25, 2015

DOI: 10.1021/acscatal.5b00492
ACS Catal. 2015, 5, 3905−3909

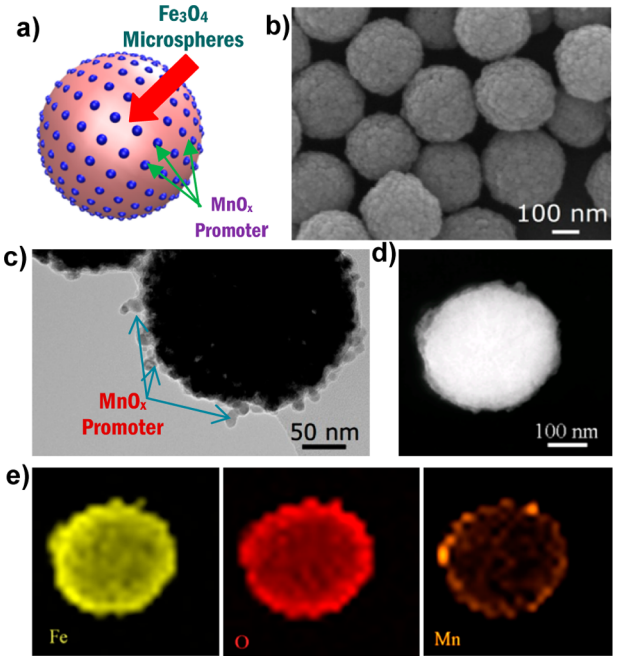

Figure 1. (a) Structural model for the Mn/Fe_3O_4 catalyst; (b) SEM images of the Fe_3O_4 microspheres; (c) TEM images of the 6 wt % Mn/Fe_3O_4 catalyst after reduction; (d) Original STEM image of the 6 wt % Mn/Fe_3O_4 catalyst as prepared; and (e) corresponding STEM-EDX elemental mapping of Fe, O, Mn on the catalyst.

carbonaceous species. The relationship between the different iron carbides and the formation of light olefins are established by several characterization methods.

The Fe_3O_4 microspheres in this work were prepared by a solvothermal method.[26a] For preparation of the Mn/Fe_3O_4 catalyst, an ethylene glycol solution of $Mn(NO_3)_2{\cdot}4H_2O$ was impregnated onto the Fe_3O_4 microspheres,[26b] followed by drying at 473 K under vacuum. Figure 1b shows SEM image of the Fe_3O_4 microspheres, which possess a uniformly spherical shape of ~300 nm. The XRD pattern (Figure S1) reveals that the microspheres are composed of magnetite. N_2 adsorption−desorption isotherms show representative type-II curves, which is normally obtained with nonporous adsorbents[26c] (Figure S2). The BET surface area and total pore volume of the microspheres are calculated to be 23 $m^2{\cdot}g^{-1}$ and 0.081 $cm^3{\cdot}g^{-1}$, respectively. These findings suggest that no pores existed inside the Fe_3O_4 microspheres. Meanwhile, it was found that the MnO_x located at the edge of Fe_3O_4 microspheres, as shown in Figure 1c. Hence, MnO_x should locate on the surface of the Fe_3O_4 microspheres as designed, and diffusion limitation in the conventional catalysts can be ignored in this catalyst system. Figure 1d,e shows the original STEM image and corresponding EDX elemental mapping of the 6 wt % Mn/Fe_3O_4 catalyst as prepared, which demonstrate the actual distribution of Fe, O, and Mn elements, separately. The Mn element can be detected mainly at the edge of Fe_3O_4 microspheres, indicating that the MnO_x locates on the surface of Fe_3O_4 microspheres. Moreover, the XPS results (Figure S3) further demonstrated that the Mn promoter located on the surface of Fe_3O_4 microspheres and the Fe−Mn interaction on the surface of Fe_3O_4 microspheres was formed for Mn-promoted catalysts. In addition, the Mössbauer spectroscopy results (Table S1 and Figure S4) indicated that incorporation of Mn has no effect on the crystal structure of Fe_3O_4 microspheres.[27] Therefore, it is considered that this unique promoter-on-iron structure of obtained catalyst would contribute to enhancing the promotional effects of manganese and clarifying the different role of iron carbides.

The prepared Fe_3O_4 microsphere catalysts were applied to FTS reaction under 1.0 MPa, 593 K, and H_2/CO ratio of 1. All the catalysts exhibited an initial increase in activity and the unpromoted Fe_3O_4 catalyst realized the highest CO conversion, as shown in Figure S5. As summarized in Table 1, the unpromoted Fe_3O_4 catalyst provided a 47% CO conversion and the 19.6% selectivity of CH_4, as well as 35.3% selectivity of C_2−C_4 olefins. Meanwhile, the molar ratio of olefin to paraffin (denoted as O/P) in the C_2−C_4 range hydrocarbons was as low as 2.5. For the 3 wt % Mn/Fe_3O_4 and 6 wt % Mn/Fe_3O_4 catalysts, the CH_4 selectivities decreased to 13.4% and 9.7%, respectively, while the C_2−C_4 olefins selectivity significantly increased to 49.5% and 60.1%, respectively (Figure 2). Further increase of Mn loading to 12 wt % resulted in the increased CH_4 selectivity and the decreased selectivity of C_2−C_4 olefins.

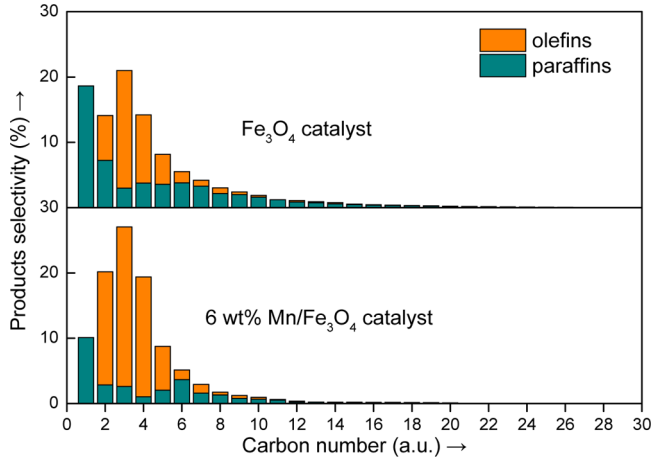

Figure 2. Product distribution of the iron-based catalysts after 50 h FTS reaction. Reaction conditions: catalyst 0.5 g, 593 K, 1.0 MPa, H_2/CO = 1, W/F (CO + H_2 + Ar) = 5 g-cat. h mol^{-1}.

Table 1. Fischer−Tropsch Synthesis Performance Data of Iron-Based Catalysts with Different Mn Loading[a]

			hydrocarbon selectivity[c] (c-mol %)				
catal.	CO conv. (%)	CO_2 sel. (%)[b]	CH_4	C_2−C_4 olefins	C_2−C_4 paraffins	C_{5+}	O/P[d]
Fe_3O_4	47.0	42.7	19.6	35.3	14.0	31.1	2.5
3 wt % Mn/Fe_3O_4	48.3	41.2	13.4	49.5	6.3	30.8	7.9
6 wt % Mn/Fe_3O_4	41.5	37.8	9.7	60.1	6.5	23.7	9.2
12 wt % Mn/Fe_3O_4	31.4	34.0	15.4	53.5	6.6	24.5	8.1

[a]Reaction conditions: catalyst 0.5 g, 593 K, 1.0 MPa, H_2/CO = 1, W/F (CO + H_2 + Ar) = 5 g-cat. h mol^{-1}. [b]Calculated from TCD, hydrocarbon free. [c]Calculated from FID. [d]The molar ratio of olefin to paraffin in the C_2−C_4 range hydrocarbons.

DOI: 10.1021/acscatal.5b00492
ACS Catal. 2015, 5, 3905−3909

It is considered that the increased Mn loading up to 12 wt % covered more surface iron atom and decreased the amount of active sites, resulting in relatively poor reaction performance. Furthermore, for the 6 wt % Mn/Fe_3O_4 catalyst, the O/P value is up to 9.2, which is much higher than previously reported results (Table S2). Meanwhile, the high content of 1-butene in all butene (Table S2) indicates that the nonporous Fe_3O_4 catalysts effectively reduce the second reaction of formed olefins,[24] contributing to clarifying the promotional effects of added Mn.

For the 6 wt % Mn/Fe_3O_4 microsphere catalysts, it is believed that the unprecedented efficiency of converting syngas to light olefins could be attributed to the special surface carbonaceous species. Therefore, the surface carbonaceous species were determined by in situ XPS (Figure S8). The analyses of carbon species on the activated catalysts confirmed the presence of significantly different surface carbonaceous species,[28,29] and the charge of surface carbon atom was influenced by the Mn promoter. It was found that the bond strength of Fe−C has a deep relationship with the charge of surface carbon atom;[16] meanwhile, the different structure of different iron carbides must lead to the different bond strength of Fe−C. Therefore, it is proposed that a specific carbide phase could be formed on the surface of Fe_3O_4 microsphere due to the presence of Mn promoter. Hence, the iron carbide phases were then determined by Mössbauer spectroscopy. Mössbauer spectroscopy of the various reduced catalysts (Figure 3, Table S3) shows that the unpromoted Fe_3O_4 catalyst was reduced and mainly carburized to Hägg iron carbide (χ-Fe_5C_2, 51.3% spectral contribution). The Mn-promoted samples exhibit lower total carbides contents after reduction compared to unpromoted catalyst, and lower degree of carbidization for Mn-promoted catalysts could directly result in relatively lower catalytic activities.[6] However, a new carbide phase, identified as cementite (θ-Fe_3C), was discerned when Mn was added. Moreover, the content of θ-Fe_3C species reached a maximum at the 6 wt % loading of Mn, and then decreased when Mn loading increased to 12 wt % (Figure S9). Meanwhile, the content of χ-Fe_5C_2 decreased continuously with the increased of Mn content. Such result indicates that the formation of surface carbide phases is affected by Mn.

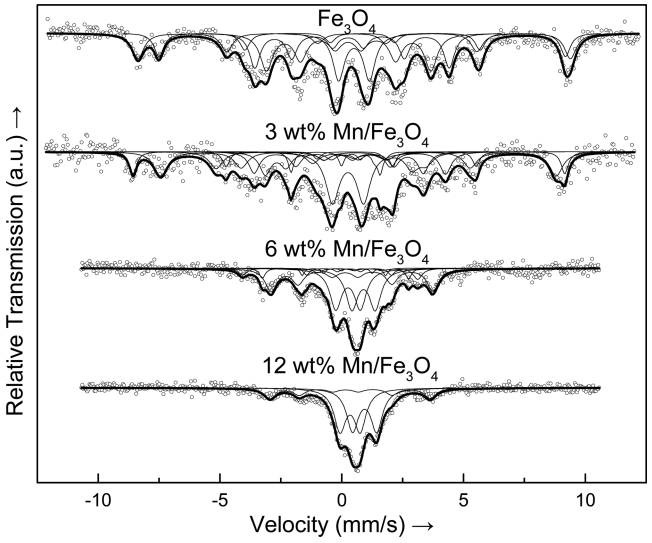

Figure 3. Mössbauer spectra of the iron-based catalysts after reduction. Reduction conditions: 623 K, 0.1 MPa, H_2/CO = 1, W/F(CO + H_2 + Ar) = 2.5 g-cat. h mol^{-1}.

To gain further information about the carbide phase, the various catalysts were characterized by XANES and EXAFS synchrotron techniques. The concentration of total iron carbides decreases with the increased Mn loading (Figure 4),

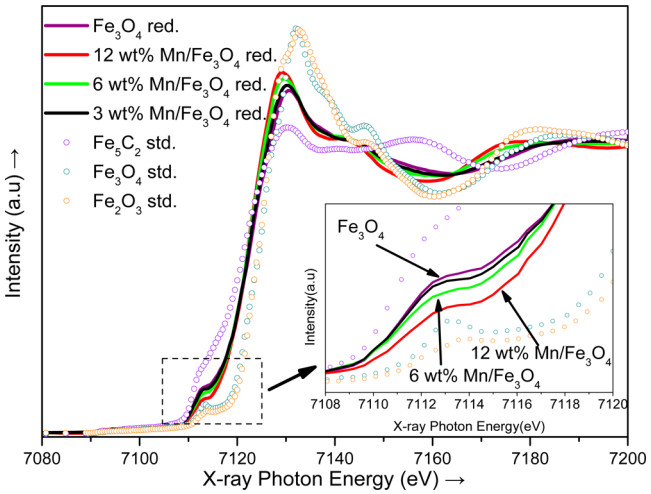

Figure 4. In situ Fe K-edge XANES of iron-based catalysts upon activation and Fe standards. All the prereduced catalysts were rereduced in situ in syngas (CO/H_2 = 1) at 623 K for 1 h.

suggesting that the carburization of the catalysts was suppressed by added Mn. This is consistent with the results from XPS and Mössbauer spectroscopy. Fourier transforms of the EXAFS spectra at the Fe K-edge (Figure 5) show that, after activation, a

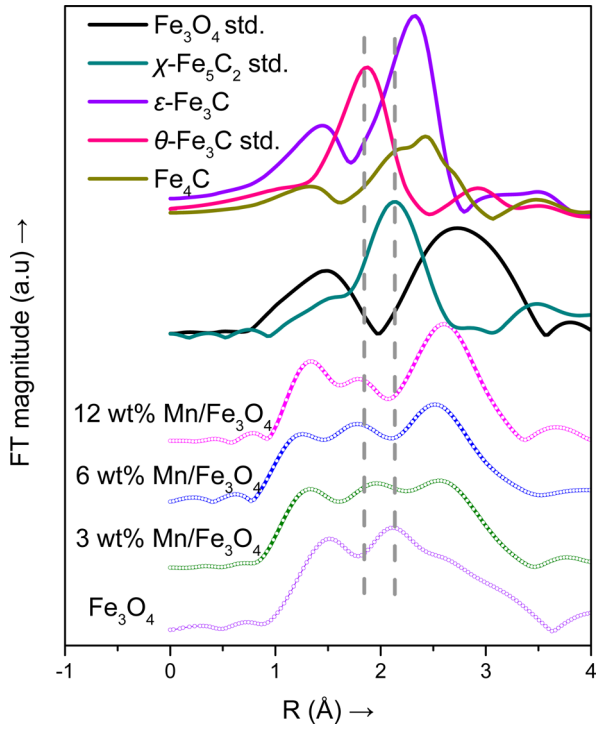

Figure 5. Fourier transformed (FT) k^3-weighted χ(k)-function of the EXAFS spectra. Solid lines denote reference samples of Fe_3O_4, χ-Fe_5C_2, ε-Fe_3C, θ-Fe_3C, and Fe_4C. All the prereduced catalysts were rereduced in situ in syngas (CO/H_2 = 1) at 623 K for 1 h.

DOI: 10.1021/acscatal.5b00492
ACS Catal. 2015, 5, 3905−3909

new scattering path appeared in the spectrum of all catalysts compared to that of fresh catalysts (Figure S11). It can be assigned to Fe−Fe path in the carbide phase, by comparing to the spectra of reference materials such as Fe_3O_4, and iron carbides.[30] Furthermore, the slightly shorter Fe−Fe bond distance (~1.8 Å) for the Mn-promoted catalysts suggests that the Fe formed another carbide phase, θ-Fe_3C, in addition to χ-Fe_5C_2.[31] Indeed, the EXAFS results together with the Mössbauer spectroscopy measurements point toward the formation of θ-Fe_3C for Mn-promoted catalysts.

Combining the above results, it is considered that a special iron carbide (θ-Fe_3C) is formed due to the promotional effects of Mn. On the other hand, the amount of θ-Fe_3C has a positive relationship with the formation of light olefins, as compared in Figure S9. The 6 wt % Mn/Fe_3O_4 catalyst, which produced highest amount of θ-Fe_3C after reduction and FTS reaction, realized the highest light olefin selectivity and O/P value in the range of C_2−C_4. Based on density functional theory (DFT) calculation results, the H_2 can easily cleave into adsorbed H and form CH_2 species, which is monomer for forming light olefins, on the Fe−C hybrid site of Fe_3C. However, the further hydrogenation of CH_2 to CH_3 and CH_4 on the site of Fe_3C needs to overcome relatively high barriers,[16] indicating that the Fe_3C phase has relatively weak hydrogenation activity for unsaturated hydrocarbon. Thus, it is reasonable to conclude that the θ-Fe_3C phase plays a crucial role in enhancing the selectivity of light olefins.

In summary, the nonporous structure combined with dispersed manganese on the Fe_3O_4 microsphere surface contributes to enhancing the promotional effects of Mn and clarifying the different role of iron carbides. Based on various characterization results, it was found that the θ-Fe_3C plays an important role to enhance the selectivity of C_2−C_4 olefins during the FTS reaction, as compared with other iron carbides. The Mn/Fe_3O_4 catalyst with a moderate amount of Mn (6 wt %) exhibits the best C_2−C_4 olefins selectivity (60.1%) and the lowest CH_4 selectivity (9.7%) with relative better stability compared with unpromoted Fe_3O_4 catalyst. In addition, this novel catalytic system proposes a new approach for obtaining a better understanding of the promotional mechanisms of the promoters.

■ ASSOCIATED CONTENT

Supporting Information

The Supporting Information is available free of charge on the ACS Publications website at DOI: 10.1021/acscatal.5b00492.

Experimental details; catalyst characterization equipment; XRD; N_2 adsorption−desorption isotherms; XPS; H_2-TPR; XAFS; Mössbauer spectra and parameters of the fresh, reduced, and used iron-based catalysts; HE-TEM micrographs for the catalysts after reduction and reaction; CO conversion as a function of time on stream; Fischer−Tropsch synthesis performance data of iron-based catalysts in our work and from other literature (PDF)

■ AUTHOR INFORMATION

Corresponding Author

*E-mail: yizhang@mail.buct.edu.cn. Tel: 86-10-64447274.

Notes

The authors declare no competing financial interest.

■ ACKNOWLEDGMENTS

Financial support from the National Natural Science Foundation of China (91334206, 51174259), Ministry of Education (NCET-13-0653), National "863" program of China (2012AA051001 and 2013AA031702) is greatly appreciated. This work was also supported by the Beijing Synchrotron Radiation Facility (BSRF) and Institute of Coal Chemistry, CAS. Special thanks to Prof. Y. Yang for Mössbauer spectroscopy.

■ REFERENCES

(1) Hu, B.; Frueh, S.; Garces, H. F.; Zhang, L.; Aindow, M.; Brooks, C.; Kreidler, E.; Suib, S. L. *Appl. Catal., B* **2013**, *132*−*133*, 54−61.
(2) Xu, J.; Zhu, K.; Weng, X.; Weng, W.; Huang, C.; Wan, H. *Catal. Today* **2013**, *215*, 86−94.
(3) Torres Galvis, H. M.; Bitter, J. H.; Khare, C. B.; Ruitenbeek, M.; Dugulan, A. I.; de Jong, K. P. *Science* **2012**, *335*, 835−838.
(4) van der Laan, G. P.; Beenackers, A. A. C. M. *Catal. Rev.: Sci. Eng.* **1999**, *41*, 255−318.
(5) Kang, J.; Cheng, K.; Zhang, L.; Zhang, Q.; Ding, J.; Hua, W.; Lou, Y.; Zhai, Q.; Wang, Y. *Angew. Chem., Int. Ed.* **2011**, *50*, 5200−5203.
(6) Chen, W.; Fan, Z.; Pan, X.; Bao, X. *J. Am. Chem. Soc.* **2008**, *130*, 9414−9419.
(7) Huo, C. F.; Wu, B. S.; Gao, P.; Yang, Y.; Li, Y. W.; Jiao, H. *Angew. Chem., Int. Ed.* **2011**, *50*, 7403−7406.
(8) Kang, J.; Zhang, S.; Zhang, Q.; Wang, Y. *Angew. Chem., Int. Ed.* **2009**, *48*, 2565−2568.
(9) Schulte, H. J.; Graf, B.; Xia, W.; Muhler, M. *ChemCatChem* **2012**, *4*, 350−355.
(10) Dong, H. H.; Xie, M. J.; Xu, J.; Li, M. F.; Peng, L. M.; Guo, X. F.; Ding, W. P. *Chem. Commun.* **2011**, *47*, 4019−4021.
(11) Li, S.; O'Brien, R. J.; Meitzner, G. D.; Hamdeh, H.; Davis, B. H.; Iglesia, E. *Appl. Catal., A* **2001**, *219*, 215−222.
(12) Nakhaei Pour, A.; Shahri, S. M. K.; Bozorgzadeh, H. R.; Zamani, Y.; Tavasoli, A.; Marvast, M. A. *Appl. Catal., A* **2008**, *348*, 201−208.
(13) Bengoa, J. F.; Alvarez, A. M.; Cagnoli, M. V.; Gallegos, N. G.; Marchetti, S. G. *Appl. Catal., A* **2007**, *325*, 68−75.
(14) Lohitharn, N.; Goodwin, J. G., Jr.; Lotero, E. *J. Catal.* **2008**, *255*, 104−113.
(15) (a) Ma, W.; Kugler, E. L.; Wright, J.; Dadyburjor, D. B. *Energy Fuels* **2006**, *20*, 2299−2307. (b) Torres Galvis, H. M.; Bitter, J. H.; Davidian, T.; Ruitenbeek, M.; Dugulan, A. I.; de Jong, K. P. *J. Am. Chem. Soc.* **2012**, *134*, 16207−16215.
(16) Huo, C. F.; Li, Y. W.; Wang, J.; Jiao, H. *J. Am. Chem. Soc.* **2009**, *131*, 14713−14721.
(17) de Smit, E.; Cinquini, F.; Beale, A. M.; Safonova, O. V.; van Beek, W.; Sautet, P.; Weckhuysen, B. M. *J. Am. Chem. Soc.* **2010**, *132*, 14928−14941.
(18) (a) Kreitman, K. M.; Baerns, M.; Butt, J. B. *J. Catal.* **1987**, *105*, 319−334. (b) Yang, Z.; Pan, X.; Wang, J.; Bao, X. *Catal. Today* **2012**, *186*, 121−127. (c) Tao, Z.; Yang, Y.; Zhang, C.; Li, T.; Ding, M.; Xiang, H.; Li, Y. W. *J. Nat. Gas Chem.* **2007**, *16*, 278−285.
(19) (a) Venter, J.; Kaminsky, M.; Geoffroy, G. L.; Vannice, M. A. *J. Catal.* **1987**, *103*, 450−465. (b) Xu, L.; Wang, Q.; Xu, Y.; Huang, J. *Catal. Lett.* **1995**, *31*, 253−266. (c) Lohitharn, N.; Goodwin, J. G., Jr.; Lotero, E. *J. Catal.* **2008**, *255*, 104−113.
(20) (a) Campos, A.; Lohitharn, N.; Roy, A.; Lotero, E.; Goodwin, J. G., Jr.; Spivey, J. J. *Appl. Catal., A* **2010**, *375*, 12−16. (b) Torres Galvis, H. M.; de Jong, K. P. *ACS Catal.* **2013**, *3*, 2130−2149.
(21) Das, D.; Ravichandran, G.; Chakrabarty, D. K. *Catal. Today* **1997**, *36*, 285−293.
(22) Morales, F.; Grandjean, D.; de Groot, F. M. F.; Stephan, O.; Weckhuysen, B. M. *Phys. Chem. Chem. Phys.* **2005**, *7*, 568−572.
(23) Maitlis, P. M.; Zanotti, V. *Chem. Commun.* **2009**, *13*, 1619−1634.
(24) Schulz, H. *Catal. Today* **2014**, *228*, 113−122.
(25) Madon, R. J.; Iglesia, E. *J. Catal.* **1993**, *139*, 576−590.

DOI: 10.1021/acscatal.5b00492
ACS Catal. 2015, 5, 3905−3909

(26) (a) Liu, J.; Sun, Z. K.; Deng, Y. H.; Zou, Y.; Li, C. Y.; Guo, X. H.; Xiong, L. Q.; Gao, Y.; Li, F. Y.; Zhao, D. Y. *Angew. Chem., Int. Ed.* **2009**, *48*, 5875−5879. (b) Lv, X.; Chen, J. F.; Tan, Y.; Zhang, Y. *Catal. Commun.* **2012**, *20*, 6−11. (c) Sing, K. S. W. *Pure Appl. Chem.* **1985**, *57*, 603−619.
(27) Li, T.; Yang, Y.; Zhang, C.; An, X.; Wan, H.; Tao, Z.; Xiang, H.; Li, Y.; Yi, F.; Xu, B. *Fuel* **2007**, *86*, 921−928.
(28) Zhang, C.; Zhao, G.; Liu, K.; Yang, Y.; Xiang, H.; Li, Y. *J. Mol. Catal. A: Chem.* **2010**, *328*, 35−43.
(29) Kang, S. H.; Bae, J. W.; Cheon, J. Y.; Lee, Y. J.; Ha, K. S.; Jun, K. W.; Lee, D. H.; Kim, B. W. *Appl. Catal., B* **2011**, *103*, 169−180.
(30) Guo, X.; Fang, G.; Li, G.; Ma, H.; Fan, H.; Yu, L.; Ma, C.; Wu, X.; Deng, D.; Wei, M.; Tan, D.; Si, R.; Zhang, S.; Li, J.; Sun, L.; Tang, Z.; Pan, X.; Bao, X. *Science* **2014**, *344*, 616−619.
(31) de Smit, E.; Beale, A. M.; Nikitenko, S.; Weckhuysen, B. M. *J. Catal.* **2009**, *262*, 244−256.

DOI: 10.1021/acscatal.5b00492
ACS Catal. 2015, 5, 3905−3909